STATUS UPDATE OF PERMANENT MAGNET RADIATION RESILIENCY STUDIES AT CEBAF*

R. M. Bodenstein†, C. Decker, K. E. Deitrick, B. R. Gamage, J. F. Gubeli, D. Hamlette, M. Janak, K. Jordan, S. Lee, C. Matthews, M. X. Mason, J. Meyers, B. Mosbrucker, I. Neththikumara, E. Nissen, V. Okey-Ejiowhor, J. Samari, S. Shriner, M. Smith, A. Ramirez, D. Thomas, N. Wilson
Thomas Jefferson National Accelerator Facility, Newport News, VA, USA
S. J. Brooks, Brookhaven National Lab, Upton, NY, USA
S. Boogert, Cockcroft Institute, Daresbury, UK
W. Shields, Royal Holloway University London, Egham, UK
B. Shepherd, STFC, Daresbury, UK

Abstract

The proposed CEBAF energy upgrade incorporates Fixed-Field Alternating-gradient (FFA) arcs utilizing permanent magnets. Validating their long-term stability in the tunnel's radiation environment is critical for technical feasibility. We present an overview of Jefferson Lab's permanent magnet radiation resiliency program, reviewing the in-situ demagnetization monitoring methodology and initial operational results. We also discuss upgrades for the ongoing second exposure campaign, which target refined dose correlations and reduced systematic uncertainties. Finally, we outline the roadmap for certifying permanent magnet optics for the upgrade energies.

INTRODUCTION

The FFA@CEBAF energy upgrade study proposes increasing the beam energy beyond 20 GeV by replacing conventional electromagnetic arcs with permanent-magnet FFA arcs [1]. Understanding the long-term radiation stability of these magnets in the CEBAF tunnel is critical for the project's technical feasibility. Radiation-induced demagnetization is a well-studied phenomenon in accelerator contexts, particularly for undulator magnets at light sources [2]. The established damage hierarchy ranks protons as most damaging, followed by neutrons, electrons, and gammas [3, 4]. However, prior studies typically relied on small sample sets ($N \leq 12$), doses far exceeding the CEBAF environment, or single material families. This LDRD project addresses all three limitations by deploying 60 sample plates carrying 540 individual magnets (spanning two NdFeB and two SmCo grades) in the operational tunnel for 12 months. An additional 57 plates serve as unexposed laboratory controls. Co-locating radiation-sensitive NdFeB with radiation-hard SmCo on each plate enables a gain-immune intra-plate differential measurement that cancels instrumental drift and isolates radiation-induced changes. This paper reports preliminary results from the first data-taking campaign and preparations for the second. Prior publications [5–7] detail the experimental design, dosimetry, simulations, and measurement apparatus.

EXPERIMENTAL OVERVIEW

Sample Design

Thirty Y-plates, each carrying four randomized permanent magnet samples (two NdFeB grades: N42EH and N52SH; two SmCo grades: SmCo33H and SmCo35), were deployed at eight tunnel regions (four recirculating arcs, two linacs, and two labyrinths) for approximately 12 months. Nine identical Y-plates remained in the laboratory as unexposed controls. The randomized co-location of all four materials on each plate is central to the analysis: the intra-plate differential between the radiation-sensitive NdFeB and radiation-hard SmCo cancels the dominant Helmholtz coil gain drift (± 0.124 %) by construction, enabling sub-percent detection sensitivity.

Additionally, pair assemblies (H-plates) with controlled magnetic configurations (aligned, antiparallel, and perpendicular) approximate different field orientations within a Halbach array [8, 9], providing data relevant to multifunction FFA magnet design.

Measurement and Dosimetry

Magnetic moments are measured with a precision Helmholtz coil system [10] and point fields with a Senis 3MH6 Teslameter [11], both mounted on mobile carts for in-situ tunnel access during accelerator downtime [12, 13]. Each plate is tracked with co-located dosimetry: optically stimulated luminescence (OSL) area monitors for photon and neutron dose, and FWT-70 optichromic rods for high-dose gamma fields [5]. Gamma doses span five orders of magnitude, from 0.3 Gy (labyrinths) to 23,000 Gy (linac positions).

FIRST CAMPAIGN RESULTS

Headline Result

Table 1 and Fig. 1 show the per-material results. Both NdFeB grades exhibit negative shifts (demagnetization), while both SmCo grades are consistent with zero, as the thermal

* Authored by Jefferson Science Associates, LLC under U.S. DOE Contract No. DE-AC05-06OR23177. The research described in this work was conducted under the Laboratory Directed Research and Development Program at Thomas Jefferson National Accelerator Facility for the U.S. Department of Energy.
† ryanmb@jlab.org

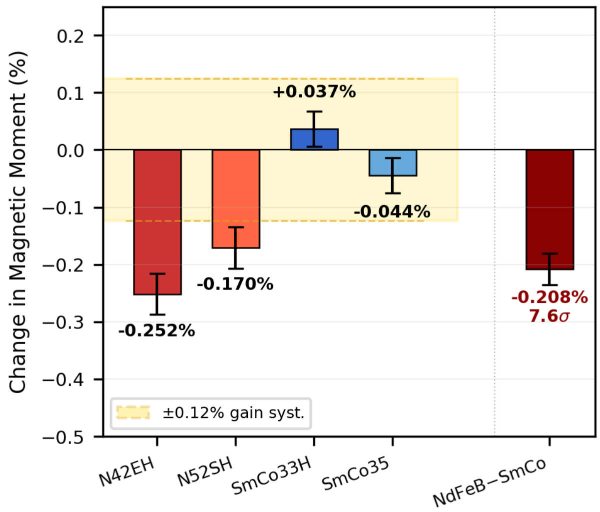

Figure 1: Mean percentage change in magnetic moment for each material grade (30 tunnel Y-plates, temperature-corrected to 20°C). Error bars: ± 1 SEM. The rightmost bar is the gain-immune intra-plate NdFeB−SmCo differential (7.6σ). The gold band indicates the $\pm 0.12\%$ Helmholtz coil gain systematic, which cancels in the differential.

spike model predicts for SmCo's higher Curie temperature (700–850°C vs. 310–350°C) and anisotropy field.

The NdFeB-minus-SmCo intra-plate differential across 30 tunnel Y-plates is

$$\delta = -0.208\% \pm 0.028\% \text{ (stat)} \pm 0.036\% \text{ (syst)}, \quad (1)$$

corresponding to 7.6σ statistical and 4.6σ combined significance. The nine lab control plates yield a null differential of $-0.007\% \pm 0.038\%$ (0.2σ), confirming that the measurement system introduces no material-dependent bias. The tunnel-minus-lab excess is independently significant at 4.3σ.

Table 1: Per-Material Mean Change (Tunnel Y-Plates, $N = 30$)

Grade	Family	Mean Δ (%)	Stat. Sig.
N42EH	NdFeB	-0.252 ± 0.036	7.0σ
N52SH	NdFeB	-0.170 ± 0.036	4.8σ
SmCo33H	SmCo	$+0.037 \pm 0.031$	1.2σ
SmCo35	SmCo	-0.044 ± 0.031	1.4σ

Dose Correlations

Correlating the gain-immune differential with co-located dosimetry reveals a clear hierarchy (Fig. 2). Gamma dose (spanning 0.3–23,000 Gy) shows no correlation with degradation (Spearman $\rho = 0.21$, $p = 0.27$). In contrast, neutron dose correlates significantly ($\rho = 0.39$, $p = 0.03$ for the differential; $\rho = 0.46$, $p = 0.01$ for NdFeB alone). This is the first in-situ accelerator confirmation of the neutron-dominated damage hierarchy established in deliberate irradiation studies [2, 4].

The gamma null is itself a positive finding: at doses up to 23 kGy, purely ionizing radiation produces no detectable

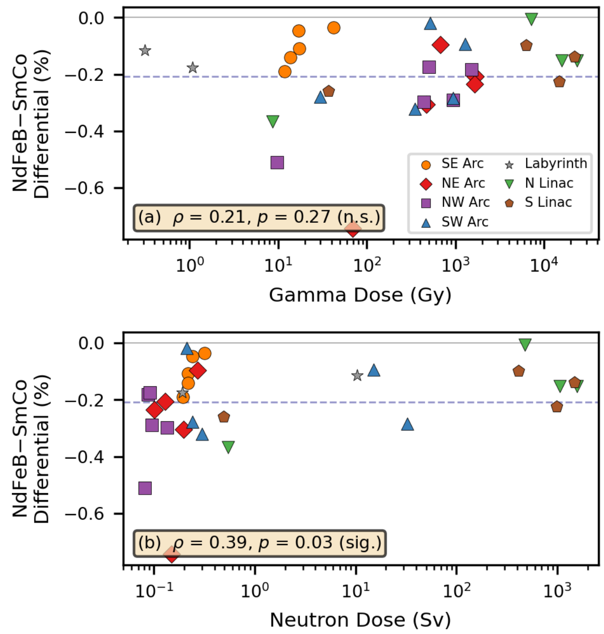

Figure 2: Gain-immune NdFeB−SmCo differential vs. (a) gamma dose and (b) neutron dose for all 30 tunnel plates. Gamma dose shows no significant correlation; neutron dose correlates significantly ($p = 0.03$), confirming the neutron-dominated damage hierarchy. Dashed line: fleet mean (-0.21%).

demagnetization, consistent with the 7 MGy gamma null reported by Alderman et al. [14]. This constrains the damage mechanism to hadronic interactions, principally nuclear displacement cascades and neutron capture.

Grade Dependence

An unexpected observation is that N42EH degrades more than N52SH, despite N42EH's higher intrinsic coercivity ($H_{ci} \geq 30$ kOe vs. ≥ 19 kOe). Composition data from the manufacturer reveals that the two NdFeB grades differ in their heavy rare-earth content, particularly dysprosium, which has a very large thermal neutron capture cross-section. We are investigating whether Dy-bearing nuclear reactions in the grain-boundary phase contribute to the observed inversion; a detailed quantitative analysis will be presented in a forthcoming publication.

SmCo shows zero degradation despite containing samarium, which also has a large neutron capture cross-section. This indicates that neutron capture alone is insufficient to cause demagnetization; the host lattice must also be intrinsically vulnerable to the resulting energy deposition. SmCo's immunity is consistent with its much higher Curie temperature and magnetocrystalline anisotropy.

IMPLICATIONS FOR FFA MAGNETS

Although the mean NdFeB degradation is 0.21%, Fig. 3 shows that individual samples span a wide range, with peak degradation reaching 0.82%. For Halbach array design, the relevant metric is not the fleet average but the worst-case

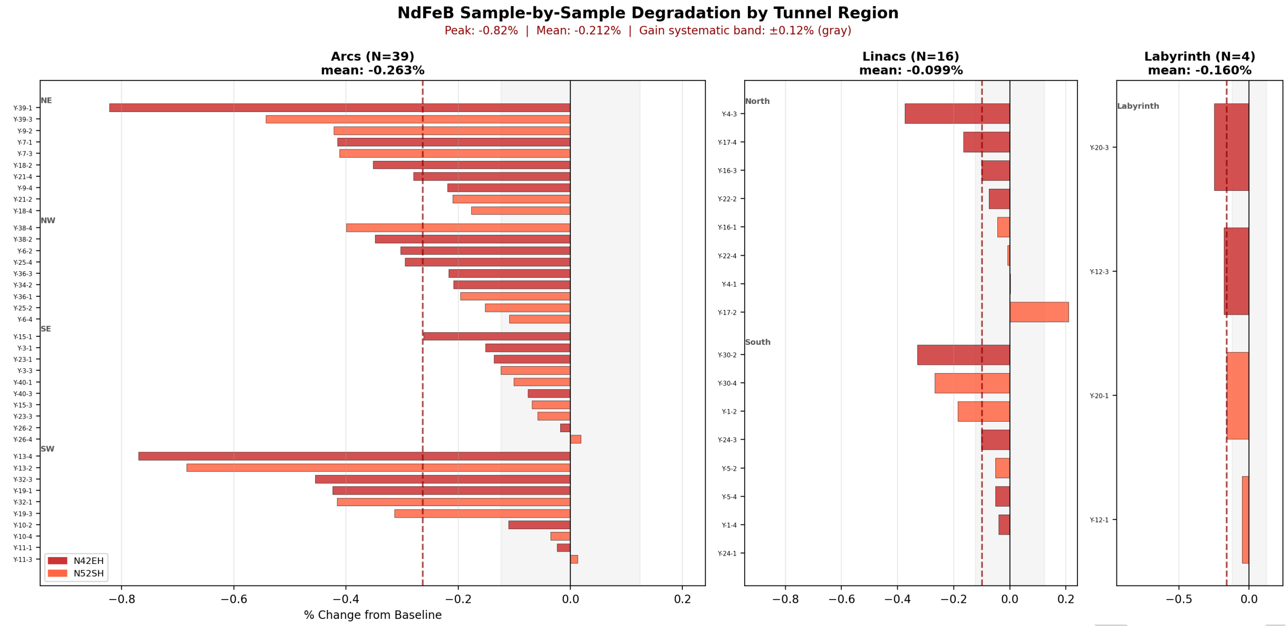

Figure 3: Sample-by-sample NdFeB degradation sorted by magnitude, grouped by tunnel region. The mean is 0.21%, but peak degradation reaches 0.82%. The gray band indicates the ±0.12% gain systematic.

wedge-to-wedge gradient across a single magnet assembly. Adjacent wedges carry reverse flux and are not equivalently exposed to the radiation field; non-uniform degradation introduces higher-order multipole errors (sextupole, octupole) that the per-sample average understates [9]. For multifunction FFA magnets, even small differential degradation between multipole components impacts the optics. With more than 70 cells per FFA arc, systematic patterns are magnified through the lattice.

Our H-plate configurations (aligned, antiparallel, perpendicular) were designed to probe orientation-dependent effects relevant to Halbach wedge geometry. Current data cannot resolve configuration-dependent differences due to baseline limitations, but this remains a priority for the second campaign.

SECOND CAMPAIGN AND OUTLOOK

The first campaign established that radiation-induced demagnetization occurs at CEBAF dose levels and is neutron-correlated. The second campaign, now underway, targets three goals:

1. **Reduce systematic uncertainties.** Multi-point baselines, improved temperature tracking, and a prospective blind analysis protocol address the dominant temperature-correction systematic (±0.033%).

2. **Establish a dose-response curve.** Integration of facility neutron detector (NDX) data [15] with per-plate dosimetry aims to produce a monotonic degradation-vs.-fluence relationship.

3. **Confirm cumulative damage.** If the differential deepens after the second exposure period, this provides definitive evidence of progressive, dose-dependent degradation.

In parallel, BDSIM simulations [16, 17] of the CEBAF beamline are progressing toward predicting the neutron fluence and energy spectrum at each plate location, enabling first-principles comparison with the measured degradation. Once validated against the current CEBAF lattice, these simulations will be extended to the upgrade energies.

CONCLUSION

This study represents the world's largest investigation of radiation-induced permanent magnet demagnetization, with 540 individual magnets deployed in the CEBAF tunnel, exceeding prior published sample sizes by an order of magnitude. The first campaign has produced a statistically significant detection of sub-percent demagnetization in a real accelerator environment, identified neutron fluence as the correlating dose quantity, and revealed an unexpected dependence on NdFeB grade that appears linked to heavy rare-earth composition. These results inform FFA magnet material selection and siting at CEBAF. The second campaign is underway with improved protocols targeting reduced systematics and a dose-response curve.

ACKNOWLEDGEMENTS

In addition to those listed as co-authors, we would like to thank the CEBAF Radiation Control Group, CEBAF Operations and Operability, and the Installation Group.

REFERENCES

[1] D. Khan *et al.*, “Current status of the FFA@CEBAF energy upgrade”, in *Proc. IPAC’24*, Nashville, TN, USA, May 2024, pp. 474–477. doi:10.18429/JACoW-IPAC2024-MOPR08

[2] T. Bizen *et al.*, "Radiation-induced magnetization reversal causing a large flux loss in undulator permanent magnets", in *Sci. Rep.*, vol. 6, 2016, p. 37937. doi:10.1038/srep37937

[3] B. Shepherd, "Radiation damage to permanent magnet materials: A survey of experimental results", in *CERN-ACC-2018-0029, CLIC-Note-1079*, CERN, 2018. https://cds.cern.ch/record/2642418

[4] A. J. Samin, "A review of radiation-induced demagnetization of permanent magnets", in *J. Nucl. Mater.*, vol. 503, 2018, pp. 42–48. doi:10.1016/j.jnucmat.2018.02.029

[5] R. M. Bodenstein *et al.*, "Permanent magnet resiliency in CEBAF's radiation environment: LDRD grant status and plans", in *Proc. IPAC'24*, Nashville, TN, USA, May 2024, pp. 3875–3878. doi:10.18429/JACoW-IPAC2024-THPS58

[6] R. M. Bodenstein *et al.*, "Current status of permanent magnet radiation resiliency studies at CEBAF", in *Proc. IPAC'25*, Taipei, Taiwan, Jun. 2025, pp. 2664–2667. doi:10.18429/JACoW-IPAC2025-THPB093

[7] R. M. Bodenstein *et al.*, "Status of permanent magnet radiation resiliency studies at CEBAF", in *Proc. NAPAC'25*, Sacramento, CA, USA, Aug. 2025, pp. 630–634. doi:10.18429/JACoW-NAPAC2025-WEAN02

[8] S. J. Brooks and S.A. Bogacz, "Permanent Magnets for the CEBAF 24GeV Upgrade", in *Proc. IPAC'22*, Bangkok, Thailand, Jun. 2022, pp. 2792–2795. doi:10.18429/JACoW-IPAC2022-THPOTK011

[9] S. Brooks, "Open-midplane gradient permanent magnet with 1.53 T peak field", in *Proc. IPAC'23*, Venice, Italy, May 2023, pp. 3870–3873. doi:10.18429/JACoW-IPAC2023-WEPM128

[10] "Model HCP Precision Helmholtz Coil Series With Rotator", https://maginst.com/products/measurement-and-testing/precision-helmholtz-coils/

[11] "3MH6 High-Precision, Low-Noise Teslameter", https://www.senis.swiss/magnetometers/teslameter-digital/3mh6-high-precision-low-noise-teslameter/

[12] E. Nissen *et al.*, "Design and instrumentation for permanent magnet samples exposed to a radiation environment", in *Proc. IPAC'24*, Nashville, TN, USA, May 2024, pp. 3879–3881. doi:10.18429/JACoW-IPAC2024-THPS59

[13] E. Nissen *et al.*, "Final design and first use of in-situ measuring apparatus for measurement of permanent magnet resiliency in CEBAF's radiation environment", in *Proc. NAPAC'25*, Sacramento, CA, USA, Aug. 2025, pp. 759–762. doi:10.18429/JACoW-NAPAC2025-WEP037

[14] J. Alderman *et al.*, "Irradiation of Nd-Fe-B with APS Bending Magnet Radiation", Argonne National Laboratory, unpublished.

[15] P. V. Degtiarenko, "Neutron detector and dose rate meter using beryllium-loaded materials", in *US Patent Number 10281600B2*, 2019, https://www.osti.gov/servlets/purl/1568305

[16] L. J. Nevay *et al.*, "BDSIM: An accelerator tracking code with particle–matter interactions", in *Comput. Phys. Commun.*, vol. 252, 2020, p. 107200. doi:10.1016/j.cpc.2020.107200

[17] B. Gamage *et al.*, "Radiation dose simulations for Jefferson Lab's permanent magnet resiliency LDRD study", in *Proc. IPAC'24*, Nashville, TN, USA, May 2024, pp. 3872–3874. doi:10.18429/JACoW-IPAC2024-THPS57